JVST A
Journal of Vacuum Science & Technology A

Selective atomic layer deposition on flexible polymeric substrates employing a polyimide adhesive as a physical mask

Cite as: J. Vac. Sci. Technol. A **39**, 012405 (2021); https://doi.org/10.1116/6.0000566
Submitted: 18 August 2020 . Accepted: 11 November 2020 . Published Online: 16 December 2020

Matin Forouzmehr, Serges Zambou, Kimmo Lahtonen, Mari Honkanen, Rafi Md Nazmul Anam, Aleksi Ruhanen, Chakra Rokaya, Donald Lupo, and Paul R. Berger

COLLECTIONS

Paper published as part of the special topic on Special Topic Collection on Area Selective Deposition ASD2020

ARTICLES YOU MAY BE INTERESTED IN

Insight into the removal and reapplication of small inhibitor molecules during area-selective atomic layer deposition of SiO_2
Journal of Vacuum Science & Technology A **39**, 012402 (2021); https://doi.org/10.1116/6.0000652

Area-selective atomic layer deposition enabled by competitive adsorption
Journal of Vacuum Science & Technology A **38**, 062411 (2020); https://doi.org/10.1116/6.0000497

Dependence of inherent selective atomic layer deposition of FeO_x on Pt nanoparticles on the coreactant and temperature
Journal of Vacuum Science & Technology A **39**, 012404 (2021); https://doi.org/10.1116/6.0000668

© 2020 Author(s).

JVST A
Journal of Vacuum Science & Technology A
ARTICLE
avs.scitation.org/journal/jva

Selective atomic layer deposition on flexible polymeric substrates employing a polyimide adhesive as a physical mask

Cite as: J. Vac. Sci. Technol. A 39, 012405 (2021); doi: 10.1116/6.0000566
Submitted: 18 August 2020 · Accepted: 11 November 2020 ·
Published Online: 16 December 2020

Matin Forouzmehr,[1] Serges Zambou,[1,2,a)] Kimmo Lahtonen,[3] Mari Honkanen,[4] Rafi Md Nazmul Anam,[1] Aleksi Ruhanen,[1] Chakra Rokaya,[1] Donald Lupo,[1] and Paul R. Berger[1,5]

AFFILIATIONS

[1]Faculty of Information Technology and Communication Sciences, Tampere University, Korkeakoulunkatu, 3, 33720 Tampere, Finland
[2]Department of Electrical and Electronics Engineering, College of Technology, University of Buea, P.O. Box 63, Buea, Cameroon
[3]Faculty of Engineering and Natural Sciences, Tampere University, P.O. Box 692, FI-33014 Tampere, Finland
[4]Tampere Microscopy Center, Tampere University, Korkeakoulunkatou, 3, 33720 Tampere, Finland
[5]Department of Electrical & Computer Engineering, The Ohio State University, Columbus, Ohio 43210

Note: This paper is a part of the Special Topic Collection on Area Selective Deposition.
[a)]**Electronic mail:** serges.zambou@tuni.fi

ABSTRACT

The rise of low-temperature atomic layer deposition (ALD) has made it very attractive to produce high-κ dielectric for flexible electronic devices. Similarly, selective deposition of ALD films is of great relevance for circuitry. We demonstrated a simple method of using a physical mask to block the film's growth in selected polymeric and flexible substrate areas during a low-pressure ALD process. A low-cost silicone adhesive polyimide tape was used to manually mask selected areas of bare substrates and aluminum strips deposited by evaporation. 190 cycles of aluminum oxide (Al_2O_3) and hafnium oxide (HfO_2) were deposited at temperatures ranging from 100 to 250 °C. Using x-ray photoelectron spectroscopy (XPS) analysis and energy dispersive x-ray spectroscopy (EDS), we showed that the mask was effective in protecting the areas under the tape. The mask did not show any modification of shape for an exposure of 10 h at 250 °C, hence keeping the form of the masked area intact. An analysis of the unmasked area by ellipsometry (632.8 nm) and x ray shows a regular film with a thickness variation under 2 nm for a given temperature and constant refractive index. EDS, selected-area XPS, and imaging XPS show an evident change of elemental content at the interface of two areas. By XPS, we established that the structure of the films was not affected by the mask, the films were stoichiometric, and there was no effect of outgassing from the adhesive film.

© 2020 Author(s). All article content, except where otherwise noted, is licensed under a Creative Commons Attribution (CC BY) license (http://creativecommons.org/licenses/by/4.0/). https://doi.org/10.1116/6.0000566

I. INTRODUCTION

Atomic layer deposition (ALD) is a thin film deposition technique that has increased in popularity in recent years. ALD is a vapor phase deposition technique that allows the production of very conformal and uniform films in a large area. This technique is based on a series of self-limiting reactions during which materials in their vapor phases are pushed alternatively into the reaction chamber at very low pressure.[1,2] The deposition starts upon chemisorption of an initial reactant or a precursor onto a substrate, usually enabled by a radical's existence, which will act as a nucleation point on the substrate. Once initiated, the reaction continues in a self-limiting manner alternated by a purge with an inert gas. In theory, the film resulting from ALD is very conformal, uniform, and default-free, and grows at a linear rate.[3] However, in practice, the film's quality is affected by several factors, including the

© Author(s) 2020

precursors' type, purge time, pulse times, reactor temperature, and equipment.[4–6] Due to their immense success, ALD protocols have been progressively used to produce binary, ternary, and quaternary compounds, metals, and even more complex materials.[7–13]

In nano and microelectronics, circuits and devices need interconnection between different layers or parts of a circuit. For instance, a connection between a gate and source-drain electrodes is required across different layers for a unipolar inverter. In large areas and flexible electronics that operate mostly with inks and solution processes, the need for interconnections, passivation, and encapsulation is of great importance. ALD layers are normally deposited as a blanket film that grows everywhere on the substrate and its surroundings, hence entirely covering any previously deposited materials. In devices and circuit fabrication, the need for interconnects requires that some part of the substrate be free of the ALD film to allow interconnection. The mechanism to achieve such results is referred to as area selective ALD (ASALD). Some approaches that have been reported are (i) a self-assembled-monolayer (SAM) that is selectively applied on the substrate to deactivate certain areas and inhibit the nucleation and growth of the thin film.[14,15] However, this comes with some difficulties, as the SAM action relies on the surface composition of the substrate or previous films, hence the difficulty of finding suitable SAMs for nontraditional substrates and films. (ii) An appropriate resist combined with photolithography and etching processes is used to achieve the desired results.[16] These methods yield high precision and resolution, which are highly desirable in nano and microfabrication; however, they are time-consuming and often difficult to achieve on polymeric substrates.[17]

For microelectronic circuits, lift-off techniques are often preferred, as they are of low cost and are more straightforward. Similarly to lift-off, several physical techniques have been employed for ASALD. For instance, in their studies, Astaneh *et al.*[18] used a pair of magnet and iron powder. They sandwiched the substrate between iron powder and a magnet that held the iron in the area with no intention to grow a film. This method was sufficient to create patterns with feature size as small as 0.3 mm on any substrate. However, this method is not suitable for reactors, sample holders, or other prepatterned parts of the circuit having magnetic properties; additionally, having iron powder in a vacuum system could be hazardous or could create messiness should the magnet fold out of place. Sweet *et al.*[19] used a pair of aluminum metal plates with the front plate open on areas where the film is needed. Their technique was successfully used to deposit ZnO on nonwoven textiles and fabrics selectively. Their study used compression force to clamp the metals and restricted the deposition area but the edge was poorly defined. Focusing on large-area ASALD, Zhang *et al.*[20] used Parafilm™ to selectively grow Al_2O_3, titanium oxide (TiO_2), and iridium of size 1 × 1 cm on a silicon substrate, but the limitation of this work was the low heat tolerance of Parafilm™ and some film penetration under the mask. In another study, Langston *et al.*[21] employed three materials (Teflon, silicon, and copper) shaped as windows with various inner and outer diameters to grow lead sulfide (PbS), aluminum oxide (Al_2O_3), zirconium oxide (ZrO_2), and platinum films onto silicon wafers selectively. In general, the clearance between the substrate and the mask should be in the nanometer order to prevent growth.[22] The silicon mask showed a film penetration of 200 nm and the copper a diffusion of 1 mm underneath the mask. These masks were made of polished plates and springs. Hence, the mask's surface smoothness, the quality of the springs, and other mobile parts could affect the clearance/gap between the substrate and the mask. The pioneering works referenced above demonstrated the working principle of a physical mask; however, none of them cover masking on flexible and polymeric substrates, widely used in modern electronics and smart packaging.

Low-temperature ALD processes have increased the interest in using the technology in soft and flexible electronics. Flexible and soft substrates are usually made of polymers with limited temperature stability. In this work, we investigate polyimide tape as an effective mask for low-pressure (<10 mbar) ASALD on polymeric substrates. We deposited Al_2O_3 and HfO_2 thin films at temperatures ranging from 100 to 250 °C and pressure on the partially masked Kapton™ substrate or aluminum strips predeposited on a polymeric substrate. SEM, energy dispersive x-ray spectroscopy (EDS), x-ray photoelectron spectroscopy (XPS), and ellipsometry were subsequently used to demonstrate Kapton tape's effectiveness as a masking element. Among other advantages, Kapton™ tape is of low cost and is widely available, and does not need any special treatment to be applied or removed from the substrate. A solvent easily removes the residual adhesive left on the substrate. Kapton™ tape also displays good temperature stability below 250 °C and does not suffer from shape distortion.

II. EXPERIMENT

Polymeric substrates are of great importance in flexible electronics for their lightweight, low cost, and mechanical properties. Among those, polyimides are the most widely used for their chemical and thermal stability. In this work, polyimide films (Kapton™ PV9100) from DuPont were used as substrates. The substrates were cut into pieces of $25 \times 25\,mm^2$, cleaned in de-ionized water, acetone, and ethanol, and sonicated in those solvents, and then blown dry with air. The substrate's back was attached to a glass slide to reinforce its stability during the manipulation and ensure that the substrate stays horizontal during the ALD. Throughout this work, a polyimide tape Kapton 5413, from 3M™ with silicone adhesive, was used as a masking element. The tape was applied onto the substrates using physical compression, and the back of a wafer tweezer was used to eliminate the air bubbles under the tape and ensure proper adhesion, especially around the edges between the tape and the substrate, which yields a better result than fingers or not square objects that tend to create contamination over the edge. The tape was of dimension $10 \times 25\,mm^2$ and applied in the middle of the sample. The tape was removed by initially pinching one edge with a straight, very thin tip tweezer and continuing the removal using a curve tweezer and isopropanol (IPA) gently removed residual glue when necessary.

In one experiment, Al_2O_3 films were grown at temperatures ranging from 100 to 250 °C. The film was grown from trimethylaluminum (TMA) and water (H_2O) on a Beneq TFS 200-273 tool in thermal mode. The typical thickness of a high-κ dielectric in a TFT transistor is under 20 nm; hence, we grew Al_2O_3 for 190 cycles. During the deposition, the reactants were allowed to enter the chamber for 300/600 ms, respectively, for TMA and water, alternated by purges of 1 s, using ultrahigh purity nitrogen gas (N_2).

© Author(s) 2020

In another experiment, HfO_2 films were deposited at a chamber reaction temperature from 100 to 250 °C. The Hafnium oxide layer was grown from tetrakis dimethylamino hafnium (TDMAH) (Strem Chemicals) and water. During the process, TDMAH was kept in a heated source at 65 °C, whereas the water was at room temperature. The films were grown in the thermal mode for 190 cycles, using the sequence TDMAH(2s)/N2(30s)/H_2O(1s)/N2(30s).

Aluminum is widely used for electrodes or connectors in circuits, so we demonstrated selective masking of aluminum strips. For this purpose, extra pure electronic grade aluminum pellets supplied by Kurt J. Lesker were used to deposit Al onto the substrate by E-beam evaporation (Fig. 1). Then, masking was performed using the same steps, as described above. The masking was done from edge to edge throughout the study, as shown in Fig. 1(a). However, we also demonstrated that this method of masking could be possible in an area located inside the substrate, like in Fig. 2.

The analysis was performed on the masked and unmasked areas to assess the mask's effectiveness and the films' quality. Ellipsometry at a wavelength of 632.8 nm was used to study the films' thickness across the growth area. A scanning electron microscope (FESEM, Zeiss, ULTRAplus) was used to explore the two areas, and point and line analysis coupled with EDS (Oxford Instruments X-MaxN 80 EDS) were used to investigate the interface of the two areas.

The surface composition of the ALD thin films was measured using XPS. Lens-defined selected-area XPS (SAXPS) and imaging XPS (iXPS) were performed employing a nonmonochromatized DAR400X-ray source (Al Kα, 1486.6 eV) and an Argus hemispherical electron spectrometer (Omicron Nanotechnology GmBh). The core-level spectra were collected with a pass energy of 20 eV (SAXPS) or 200 eV (iXPS) and in-lens aperture, yielding a circular analysis area of 2.93 mm^2 (SAXPS) or 0.031 mm^2 (iXPS). The in-lens deflector was utilized to scan the analysis area across the sample in 50 μm increments for recording the sweep spectrum line scans of Al 2p and Hf 4f. The lateral resolution of iXPS was 136 μm (knife-edge 16%–84%). The surface composition was identified by analyzing core-level spectra using CasaXPS software (version 2.3.19 PR 1.0).[23] Due to surface charging, the binding energy scale was calibrated according to a C 1s C−C/H peak at 284.8 eV. The background-subtracted XPS peaks were least squares fitted with mixed Gaussian–Lorentzian component line shapes. The relative atomic concentrations were calculated using Scofield photoionization cross sections and an experimentally measured transmission function of the Argus analyzer.

III. RESULTS AND DISCUSSION

The polyimide Kapton™is one of the most widely used flexible substrates in electronics for its mechanical properties, thermal

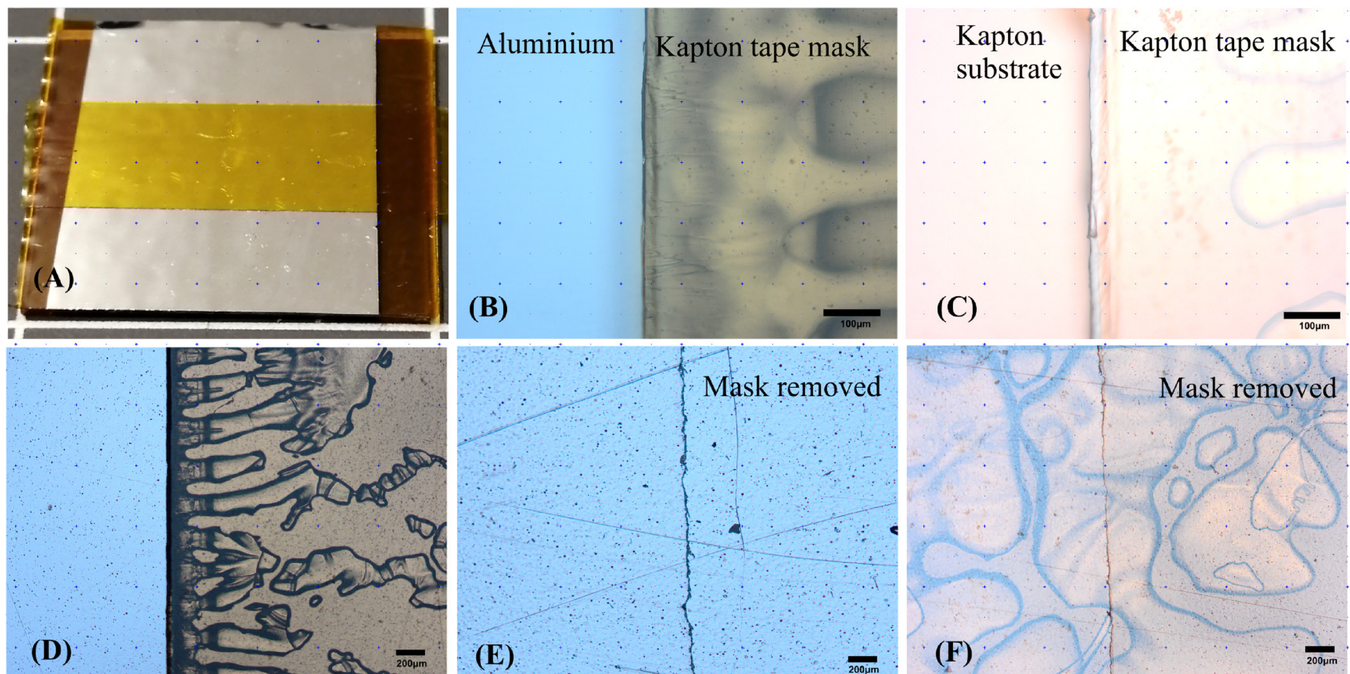

FIG. 1. (a) Photograph of a 2.5 × 2.5 cm^2 sample made of evaporated aluminum; a section of 0.9 × 2.5 cm^2 masked a selected area on the sample. The images are for an Al_2O_3 film deposited at 250 °C. (b) Optical microscopy image magnified 20 times of a small selected area at the interface between the aluminum and the Kapton masking tape. (c) Optical image at 20×, an Al_2O_3 sample grown at 250 °C, and the Kapton tape is used to mask the Kapton substrate. (d) Optical image at 5× of an area from the image (a), the sample was heated at 250 °C for 10 h in N_2 to assess the behavior of small air bubbles trapped by glue under the tape. (e) 5× optical image of (b) after the mask removal. (f) 5× optical image of (c) after the mask removal.

© Author(s) 2020

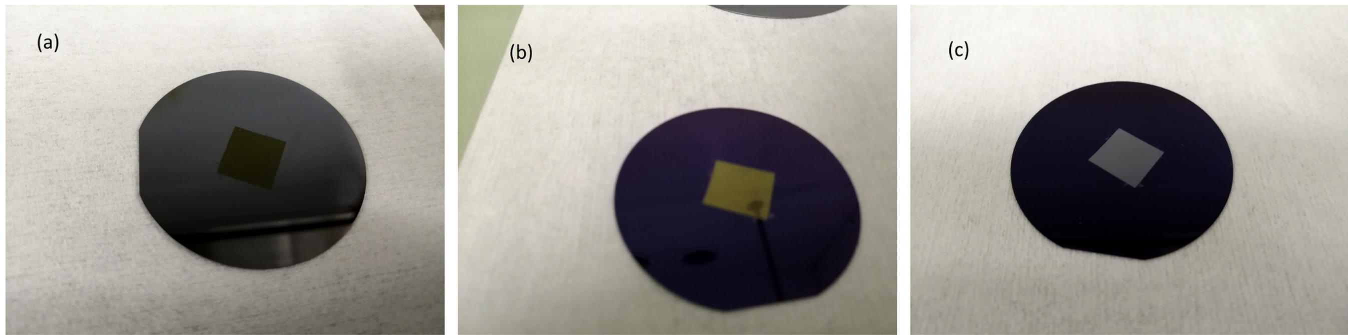

FIG. 2. Illustration of selective masking using a polyimide tape on a 2-in. silicon wafer. (a) The mask is applied on the wafer and located inside the wafer; (b) image after a 100 nm of Al_2O_3 is deposited using TMA and water at 100 °C; and (c) image after the mask has been removed.

stabilities, and low outgassing rate compared with other polyimides and polymers.[24] Kapton™ silicone adhesive tape used in this work as a masking element was first tested for dimension stability under high temperature and a very low vacuum for an extended period. A tape of dimension $0.9 \times 2.5\,cm^2$ was tightly pressed onto a bare substrate or in a 100 nm thin aluminum strip deposited by E-beam evaporation, as seen in Fig. 1(a). The silicone adhesive ensures the contact between the substrate and the mask; they have been demonstrated to be stable and work well under low vacuum and high temperature.[25] The tape was specified to work well at 350 °C. However, keeping the tape in the ALD reactor at 300 °C for more than 10 h led to the formation of bubbles under the tape.

This phenomenon was not visible even under optical microscopy for a temperature under 250 °C. Thus, subsequent experiments were limited to this temperature. The results shown in Fig. 1 are representative of the sample population. Shape modification is a concern in physical masking. Using Parafilm™ as a mask, Zhang *et al.*[20] reported a variation of 0.1 cm for the exposure of parafilm at 300 °C for 6 h. For this study, several samples were kept at 250 °C in the ALD reactor for more than 10 h, and no noticeable shrinkage or size modification was observed in any of the mask directions. In Fig. 2, we showed that this technique is not only meant for masking from edge to edge but could also be applied for areas contained inside the substrate. We illustrate this by growing 100 nm of Al_2O_3 at 100 °C on a 2-in. silicon wafer and Kapton™ tape, but for the visibility, only the wafer substrate is presented. We observed that the masked area was protected during the deposition without any noticeable distortion of shape. In Fig. 1, several images are presented; they are optical images of the Al_2O_3 film deposited growth under low vacuum at 250 °C. In Figs. 1(b) and 1(e), we used an optical microscope (Olympus BX60M) at 20× and 5×, respectively, to show the interface between the masked and the unmasked area with the mask still on and when the mask is removed. The sealing at the edge of the mask remained intact for the temperatures studied, which is an advantage compared with the use of hard masks,[19,21] and this sealing allows more influx of materials and film formation under the mask. Figure 1(c) shows the Al_2O_3 film growth; the masking tape is visible on the right side of the figure. In Fig. 1(f), the mask has been removed from Fig. 1(c) and a line is observed in both Figs. 1(e) and 1(f), representing the residue from the adhesive. Several drawbacks were also noticed upon using this method; these include the presence of residual adhesives. Even though residues were not visible in several instances, we could still detect silicon resulting from the adhesives on XPS. In some cases, where the residues were visible, we could remove them using IPA without any noticeable damage on the substrate. Nevertheless, IPA's use increases the likelihood of organic contamination, as Raghu *et al.*[26] discussed the adsorption of IPA by oxide dielectric, which in the case of HfO_2, can be completely removed at 300 °C. However, this temperature is not compatible with most polymeric and flexible substrates. Adhesive tape is known to trap air bubbles under the tape, so we investigated the behavior of such microairbubbles as the deposition temperature increases. Figure 1(d) shows a small section of Fig. 1(a) at the edge of the mask at 5×. In this case, the sample was kept in the ALD reactor chamber for more than 10 h, and we observed that the microbubbles were fusing progressively and moving toward the sealing edge. The maximum time for film growth in this study was 3 h; hence, we did not experience such a phenomenon. However, this could affect the quality of thick films, which are often grown for several days.

Further analysis was carried with electron microscopy to determine whether oxide deposition took place under the mask. This was performed for each set of temperatures; the results were similar. We used an SEM (Zeiss UltraPlus SEM) to analyze the sample on both masked and unmasked areas. Figure 3(a) from the 100 °C Al_2O_3 deposited film shows an image when the adhesive residue is left. The vertical middle line is the glue residue after the mask was removed. The adhesive residue was easily removed with IPA. In Fig. 3(b), we observe a lack of oxygen beyond the expected native oxide layer, which means Al_2O_3 did not grow under the mask. We can further observe a steep increase in oxygen content at the edge of the mask. Similarly, we observe the sudden reduction of aluminum at the same line; these results, further confirmed by XPS, implied that, at a microscopic level, there was no visible penetration of films under the mask, a positive advantage compared with previously observed residual penetration of films at a similar scale.

© Author(s) 2020

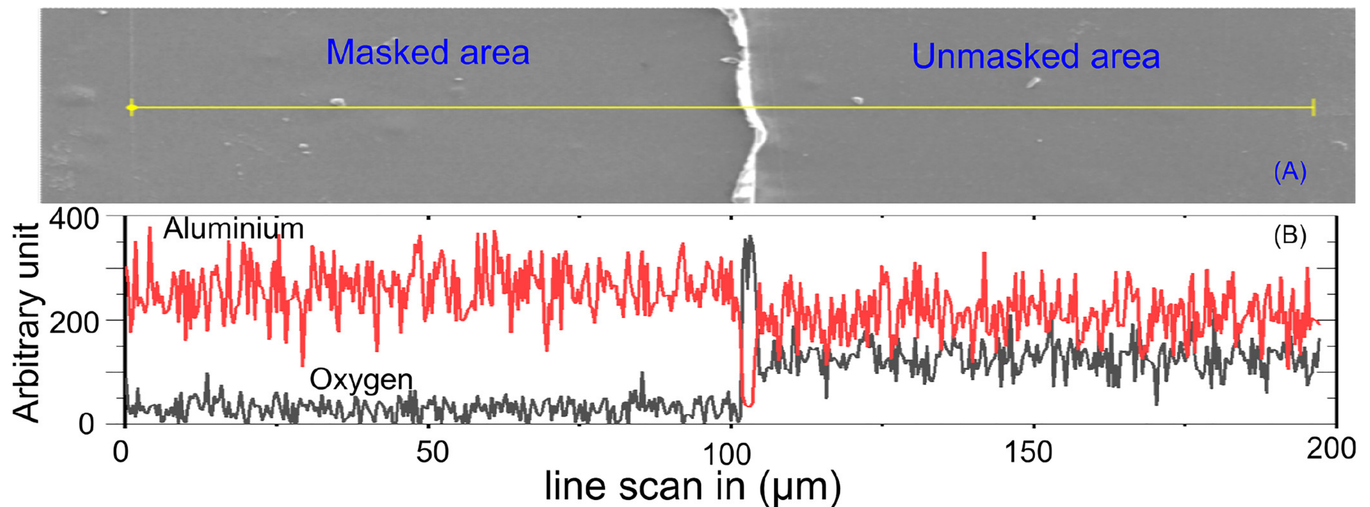

FIG. 3. Sample representation for the Al_2O_3 deposited on aluminum at 100 °C. (a) An SEM micrograph with a line scan at the interface of the masked and unmasked areas of a sample. (b) Material profiles; aluminum is the top plot and the lower is oxygen (color online).

Using SEM-EDS (Oxford Instruments X-MaxN 80 EDS), we performed the elemental analysis across the sample by using point analysis, as shown in Fig. 4. In Fig. 4(a), we focus on the elemental analysis of oxygen and aluminum deposited on the aluminum film. The peaks of the two elements, both in the masked and nonmasked areas, are superposed in Fig. 4(a). The black plot on a nonmasked area shows oxygen and aluminum close to stoichiometric proportion, as reported from various XPS studies.[27–29] For the Al_2O_3 growth on bare Kapton at 100 °C, we examine the aluminum content of the two areas using point analysis and present this in Fig. 4(b). This shows no detectable trace of aluminum under the mask and hence no film formation underneath the mask. These results were consistent at all temperatures.

The thickness of the films' growth with hafnium oxide and aluminum oxide was uniform throughout the experiment at various

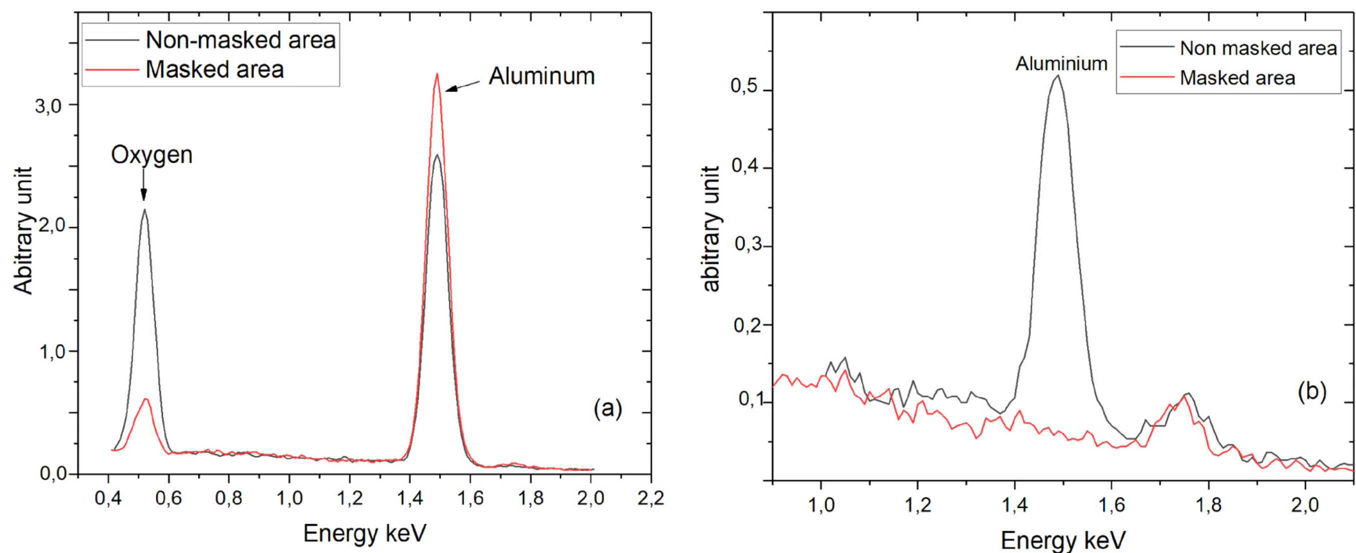

FIG. 4. (a) EDS analysis of the Al_2O_3 deposited on aluminum at 100 °C. Point analysis with the masked area showing high oxygen level; the unmasked area shows a very low oxygen level, and a high aluminum peak (color online). The peaks of oxygen and aluminum are represented at each point. (b) Point analysis of aluminum deposited on the masked and unmasked areas on a bare Kapton substrate.

© Author(s) 2020

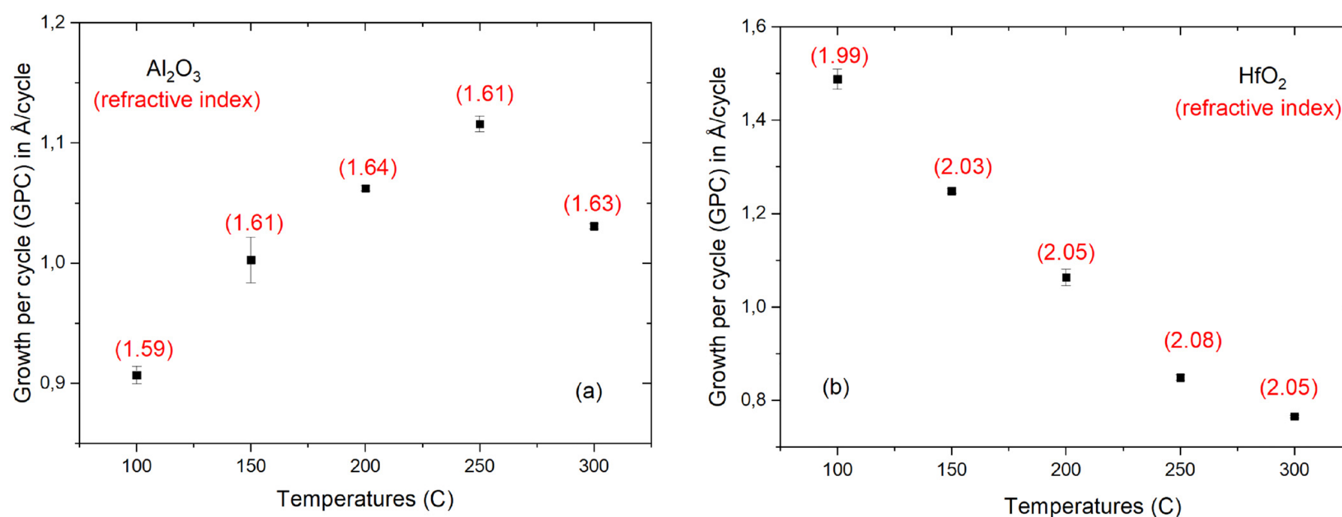

FIG. 5. GPC at various temperatures. Numbers in parentheses indicate refractive index at the given temperature. (a) Aluminum oxide. (b) Hafnium oxide.

temperatures. We used ellipsometry at 632.8 nm, measuring an average of six points from two samples deposited at the same temperature and calculating the average. The values were in a tight range, reflecting the uniform growth of the film. For instance, at 250 °C, the film thicknesses were 21.2 and 16.2 nm for Al_2O_3 and HfO_2, respectively, with standard deviations of 0.126 and 0.121 nm. In Fig. 5, we report the growth per cycle (GPC) at increasing temperatures and the standard deviations for 6 data points. The refractive indices of the films are also reported; their typical standard deviation was 0.01. These values were consistent with those in the literature on similarly grown ALD processes,[27,28,30] hence further supporting the fact that potential outgassing of the mask did not alter the film quality.

As reported in the experimental section, HfO_2 film was also deposited on Kapton and aluminum using TDMAH and H_2O. The mask was similarly effective with this film. Other residual elements such as nitrogen and silicon arose from nitrogen as the carrier gas, and a silicone adhesive use for masking was detected.

Table I shows the typical elemental content at 250 °C for a HfO_2 grown on aluminum. The weight percentage is 80 and 20 for hafnium and oxygen, respectively, when contaminants are omitted in the unmasked area. No trace of hafnium was found in the masked area. This film's stoichiometry was consistent with that of other reports of HfO_2 grown with TDMAH and H_2O.[31,32]

TABLE I. Area elemental analysis by EDS. Elemental content by percentages of weight for the masked and unmasked areas at 250 °C for a HfO_2 film deposited on aluminum.

	Element	Wt. %
Masked	Hf	80
	O	20
Unmasked	Hf	00
	O	< 5

As a direct demonstration for the use of this method for masking in large-area flexible devices where the edge between the film and the unmasked area is not critical, we fabricated an electrolytic capacitor of dimension $5 \times 5\,cm^2$. Current collectors or anodes made of PET/Al foil (Pyroll, thickness of the layers 50 and 9 μm) were used as a substrate. We deposited a 50 nm of Al_2O_3 on the aluminum foil while masking ($0.5 \times 5\,cm^2$) from one side of the electrode that would serve for probing, which otherwise would read an open circuit.

The highly conductive, stabilized ink, poly(3,4-ethylene dioxythiophene) polystyrene sulfonate PEDOT: PSS (from Heraeus), was printed on the ALD deposited film (dielectric). The ink covered an area of $4 \times 4\,cm^2$ and a 200 μm thick cure at 130 °C for 20 min. The structure was completed by depositing a metal current collector made of graphite (PF407C) with a dimension of $3.8 \times 3.8\,cm^2$ and a thickness of 150 μm. The cell led to a capacitance value of 2.066 μF and an ESR 3.62 Ω, hence demonstrating one of the useful features of this technique for flexible application.

Further analyses were performed by XPS to determine the chemical composition of the surface and further assess whether there was residual growth under the mask. A comparative study of Al_2O_3 grown on pristine silicon (used as the reference) and Kapton substrate at 250 °C was performed to ensure that the films on Kapton were of good quality and that potential outgassing,[20] which was known to occur with some polymeric substrates, does not affect the film as reported by Battes *et al.*[24] The two films' XPS survey spectra show mainly Al and O with F and C as contaminants. The main elements were in similar proportion in the two films; we attributed the presence of carbon and fluorine to the likely contamination during the ALD process or to exposure and handling from the ALD to the XPS reactor chamber. The oxygen and aluminum peaks correspond to typical Al_2O_3 oxide growth by ALD.

© Author(s) 2020

TABLE II. Binding energy in (eV) for species on unmasked and masked areas of a deposited Al_2O_3 deposited on aluminum at 250 °C.

	F 1s	O 1s		C 1s				Si $2p_{3/2}$				Al 2p	
Deconvolution	F^-	O–Al/–C/=C	O–Si	C–C/H	C–O(–C/H)	C=O	O–C=O	Si^+	Si^{2+}	Si^{3+}	Si^{4+}	Al^0	Al^{3+}
Unmasked	686.1	531.6	533.0	284.8	286.5	—	289.9	99.9	—	102.1	—	—	74.4
Masked	—	531.6	532.9	284.8	286.1	287.7	289.5	—	—	101.8	103.4	72.0	74.7

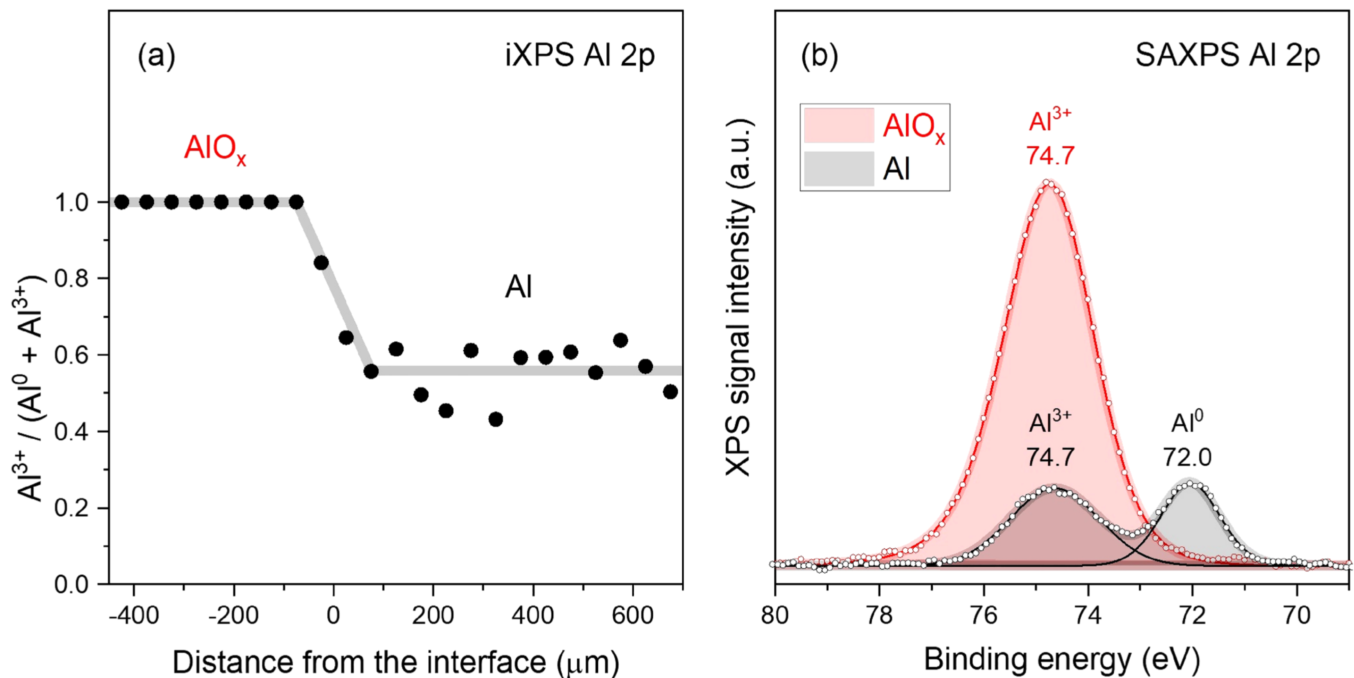

FIG. 6. (a) iXPS Al 2p line scan over the AlO_x/Al interface showing the $Al^{3+}/(Al^0+Al^{3+})$ ratio. The line is drawn to guide the eye only. (b) SAXPS Al 2p measured 2 mm away from the interface on both AlO_x and Al sides of the sample. The $Al^{3+}/(Al^0+Al^{3+})$ ratio was 0.58 on the Al side of the sample. Approximately, the same oxide/metal ratio was observed in the line scan up to the interface.

TABLE III. Binding energy in (eV) for species on unmasked and masked areas of a deposited Al_2O_3 deposited on Kapton. The film was deposited at 250 °C.

	C 1s			N 1s		O 1s		F 1s	Al 2p		Si $2p_{3/2}$				Ca $2p_{3/2}$
Deconvolution	C–C/H	C–O(-C/H), C-N	O/N-C=O	N–X	N–C	O–Al/-C/=C	O–Si	F^-	Al^0	Al^{3+}	Si^+	Si^{2+}	Si^{3+}	Si^{4+}	Ca^x
Unmasked	284.8	286.6	290.0	—	—	531.7	532.8	686.0	—	75.0	100.0	-	102.3	-	-
Masked	284.8	286.0	288.6	398.5	400.5	532.9	533.1	—	—	—	—	—	101.8	103.3	347.5

© Author(s) 2020

TABLE IV. Binding energy in (eV) for species on unmasked and masked areas of a deposited HfO_2 deposited on aluminum. The film was deposited at 250 °C.

	C 1s			O 1s			Al 2p		Si $2p_{3/2}$				Hf $4f_{7/2}$	
Deconvolution	C−C/H	C−O(−C/H)	O−C=O	O−Hf	O−Al/−C/=C	O−Si	Al^0	Al^{3+}	Si^+	Si^{2+}	Si^{3+}	Si^{4+}	Hf^{2+}	Hf^{4+}
Unmasked	284.8	286.5	289.1	530.4	—	532.4	—	—	—	101.2	—	102.7	16.8	17.6
Masked	284.8	286.5	288.7	—	531.3	532.9	72.0	74.6	—	—	101.8	103.3	—	—

An observation of the masked and unmasked areas for the Al_2O_3 film growth on aluminum strips at 250 °C shows a presence of F 1s, O 1s, C1s, Al 2p, and Si $2p_{3/2}$ peaks at energies of 686.1, 531.6, 284.8, 74.7, and 99.9 eV, respectively, as shown in Table II. An analysis of peaks and their contribution to the unmasked area gave an aluminum to oxygen ratio of 0:697, which was close to the stoichiometric value of 0.666. The binding energy value of Al 2p confirmed the existence of Al−O bonds in the Al_2O_3 film. There was no evidence of the presence of Al−Al bonds, as all detected Al was bonded to O, but the undetected O was bonded to Al. Fluorine was residual and did not appear on the masked surface. The deconvolution of the O 1*s* peak showed the existence of O−Al and O−Si bonds. These bonds were found to be present on the two surfaces with the same binding energies, but the concentration of O−Al on the masked surface was in trace amounts compared with that of the unmasked surface. The trace amount of oxide identified on the masked surface was attributed to aluminum's natural oxidation because no oxygen was found on a sample run on bare Kapton, whereas the deconvolution of C 1*s* demonstrated the existence of C−C as the strongest bond with the additional presence of C−O and O − C = O bonds associated with incompletely decomposed precursors.[29]

Imaging XPS was performed 2 mm away from the interface on the masked and unmasked areas to test the blurring interface. We observed different surfaces, which confirms the effectiveness of the adhesive tape masking approach. The unmasked area does not contain any metallic Al, and the masked side is mostly metallic Al, plus a thin oxide layer resulting from natural oxidation. The masked side was very uniform in the aluminum oxide/metal ratio up to the interface. The oxide to metallic ratio is approximately the same far away from the interface (measured with SAXPS) and close to the interface (iXPS line scan), Fig. 6(a). Figure 6(b) shows an SAXPS measurement done 2 mm away from the interface.

Further analysis of films deposited on Kapton (Table III) corroborates the results already obtained on aluminum strips. The deconvolution of the Al 2p peak shows the existence of aluminum Al^{3+} on the unmasked area at 75.0 eV binding energy, which represents a slight shift of 0.3 eV compared with the film's growth on the aluminum strip. The elemental content of aluminum and oxygen concentration at the unmasked area's surface remains similar to that of the film deposited on aluminum. The O 1s peak's deconvolution is also consistent with that of the Al_2O_3 film deposited on aluminum. An analysis of the masked area shows no trace of Al $^{3+}$ or Al ^{0}, which means no film is built under the mask. However, the masked area shows oxygen in low quantity with binding energies of 532.5 and 533.1 eV, corresponding to O−Al/−C/=C and O−Si bonds, respectively. This was attributed to the presence of oxygen at the surface of the polyimide use.

To ensure that the result was not specific to the case of Al_2O_3, we used the same analysis for the HfO_2 film growth at 250 °C on aluminum, as shown in Table IV. In this case, we observed O 1*s*, C 1*s*, Si $2p_{3/2}$, Al 2p, and Hf $4f_{7/2}$ peaks at energies of 530.4, 284.8, 101.2, 72.0, and 16.8 eV, respectively, as shown in Table IV. Further analysis of Al 2p peaks on the two areas shows the presence of metal aluminum Al^0 and a slightly thin oxidized layer translated by the presence of Al^{3+} on the masked area, whereas the unmasked area shows no trace of aluminum. This agrees with the results of aluminum oxide films. The deconvolution of O 1*s* shows binding energy at 530.4 eV for the unmasked area, corresponding to the bond O−Hf and a different one at 531.3 eV on the masked area, corresponding to O−Al bonds. Hafnium was observed at two energy levels of 16.8 and 17.6 eV corresponding to the bond created by hafnium Hf^{2+} and Hf^{4+}, and no trace of hafnium on the masked side was found, which further confirms the effectiveness of the masking.

IV. SUMMARY AND CONCLUSIONS

In this work, a polyimide tape with a silicone adhesive is used to successfully perform area selective ALD in flexible substrates. The tape was manually pressed onto a bare substrate or a 100 nm thick layer of aluminum. Throughout the study, 190 cycles of Al_2O_3 and HfO_2 corresponding to various thicknesses at a given temperature were used. Films were deposited by ALD at various temperatures ranging from 100 to 250 °C. After the deposition, the tapes were removed, and the masked and unmasked areas of the sample were studied using optical microscopy, electron microscopy, EDS, XPS, and ellipsometry. We first showed that our mask dimensions did not vary while being kept for more than 10 h at 250 °C in the ALD reactor under a low vacuum. We also found that air bubbles trapped under the tape expand outward but may take more than 10 h at 250 °C. Hence, our masking technique is safe for most conventional deposition protocols in research or industry. Using SEM images and EDS line scans of the sample, we showed no film growth under the tape, i.e., our technique was efficient in masking ALD deposition onto a polymeric substrate onto conductive material such as aluminum. Using XPS, we further demonstrated that the films were properly formed and that their chemical content was similar to that of previously reported films, close to the stoichiometric ratio, and that no contamination from mask outgassing occurred. XPS further revealed no film growth under the mask and regular film quality in the two areas. Hence, we conclude that mechanical lift-off by a polyimide adhesive tape is a viable technique to mask flexible substrates for low-vacuum, low-temperature ALD deposition selectively. As a perspective, it is understood that additional images, for instance, with a high-resolution tunneling

© Author(s) 2020

electron microscope, may have provided different pieces of information on the interface between the film and the broken tape and could help in understanding how the tape is removed.

ACKNOWLEDGMENTS

This project was supported by the Academy of Finland (AoF) under the project HiFlex (No. 31213264243 SA) hosted by Tampere University and by the European Union's Horizon 2020 Research and Innovation Program under the Marie Skłodowska–Curie Grant Agreement No. 814299—CHARISMA. The views expressed in the manuscript and the content are those of the authors and not of the funding agencies. The authors made use of the Tampere Microscopy Center facilities at Tampere University for their electron microscopy work.

DATA AVAILABILITY

This study's raw data were generated at various facilities (microscopy center, XPS facilities, Future Electronic Laboratory) at Tampere University. The data are images, Docx, excel, and original files. The data that support the findings of this study are available from the corresponding author upon reasonable request.

REFERENCES

[1] S. M. George, Chem. Rev. **110**, 111 (2009).
[2] R. W. Johnson, A. Hultqvist, and S. F. Bent, Mater. Today **17**, 236 (2014).
[3] J. S. Ponraj, G. Attolini, and M. Bosi, Crit. Rev. Solid State Mater. Sci. **38**, 203 (2013).
[4] H. H. Sonsteby, A. Yanguas-Gil, and J. W. Elam, J. Vac. Sci. Technol. A **38**, 020804 (2020).
[5] S. Neudeck, A. Mazilkin, C. Reitz, P. Hartmann, J. Janek, and T. Brezesinski, Sci. Rep. **9**, 5328 (2019).
[6] C. Wiegand, R. Faust, A. Meinhardt, R. Blick, R. Zierold, and K. Nielsch, Chem. Mater. **30**, 1971 (2018).
[7] J. Kropp, Y. Cai, Z. Yao, W. Zhu, and T. Gougousi, J. Vac. Sci. Technol. A **36**, 06A101 (2018).
[8] X. Meng, Energy Storage Mater. **30**, 296 (2020).
[9] A. Mackus, J. Schneider, C. MacIsaac, J. Baker, and S. Bent, Chem. Mater. **31**, 1142 (2020).
[10] M. B. E. Griffiths, P. Pallister, D. Mandia, and S. Barry, Chem. Mater. **28**, 44 (2016).
[11] Z. Guo and X. Wang, Angew. Int. Ed. **57**, 5898 (2018).
[12] A. Afif, A. Dadlani, S. Burgmann, P. Kollensperger, and J. Torgersen, Mater. Des. Process. Commun. **2**, e114 (2018).
[13] T. S. Tripathi and M. Karppinen, Adv. Mater. Interfaces **4**, 1700300 (2017).
[14] D. Bobb-Semple, K. Nardi, N. Draeger, D. Hausmann, and S. Bent, Chem. Mater. **31**, 1635 (2019).
[15] S. Seo *et al.*, ACS Appl. Mater. Interfaces **9**, 41607 (2017).
[16] A. Mackus, A. Bol, and W. Kessels, Nanoscale **6**, 10941 (2014).
[17] S. Astaneh, G. Jursich, C. Sukotjo, and C. Takoudis, Appl. Surf. Sci. **493**, 779 (2019).
[18] S. H. Astaneh, C. Sukotjo, C. Takoudis, and A. Feinerman, J. Vac. Sci. Technol. B. **38**, 025001 (2020).
[19] W. Sweet, C. Oldham, and G. Parsons, ACS Appl. Mater. Interfaces **6**, 9280 (2014).
[20] C. Zhang, J. Kalliomäki, M. Leskelä, and M. Ritala, J. Vac. Sci. Technol. A **36**, 01B102 (2018).
[21] C. Langston, T. Usui, and F. B. Prinz, J. Vac. Sci. Technol. A **30**, 01A153 (2012).
[22] J. Elam, D. Routkevitch, P. Mardilovich, and S. George, Chem. Mater. **15**, 3507 (2003).
[23] N. Fairley, CasaXPS: Spectrum processing software for XPS, AES, and SIMS, version 2.3.19PR1.0, Casa Software Ltd, 2006.
[24] K. Battes, C. Day, and V. Hauer, J. Vac. Sci. Technol. A **36**, 021602 (2018).
[25] A. Laikhtman, I. Gouzman, R. Verker, and E. Grossman, J. Spacecraft Rockets **46**, 236 (2012).
[26] P. Raghu, N. Rana, C. Yim, E. Shero, and F. Shadman, J. Electrochem. Soc. **150**, F186 (2003).
[27] S. E. Potts *et al.*, J. Electrochem. Soc. **158**, C132 (2012).
[28] Z. W *et al.*, Nanoscale Res. Lett. **10**, 46 (2015).
[29] I. Iatsunskyi, M. Kempiński, M. Jancelewicz, K. Załęski, S. Jurga, and V. Smyntyna, Vacuum **113**, 52 (2015).
[30] M. Aguilar-Gama, E. Ramirez-Morales, Z. Montiel-Gonzalez, A. Mendoza-Galvan, M. Sotelo-Lerma, P. Nair, and H. Hu, J. Mater. Sci. Mater. Electron. **26**, 5546 (2015).
[31] R. Lo Nigro, E. Schilirò, G. Mannino, S. Di Franco, and F. Roccaforte, J. Cryst. Growth **539**, 125624 (2020).
[32] M. Kotilainen, R. Krumpolec, D. Franta, P. Souček, T. Homola, D. Cameron, and P. Vuoristo, Sol. Energy Mater. Sol. Cells **166**, 140 (2017).

© Author(s) 2020